Chapter 16

Collisions among molecules can also be viewed as a problem in time-dependent quantum mechanics. The perturbation is the "interaction potential", and the time dependence arises from the movement of the nuclear positions.

The simplest and most widely studied problems in chemical reaction dynamics involve describing the unimolecular motion or bimolecular collision of a system in a well characterized electronic state. Referring back to the discussion of Chapter 3, we recall that the motion of the nuclei are governed by a Schrödinger equation

$$[E_j(R) \quad {}_j{}^0 (R) + T \quad {}_j{}^0(R)] = E \quad {}_j{}^0 (R)$$

in which the electronic energy $E_j (R)$ assumes the role of the potential upon which movement occurs. This treatment of the nuclear motion is based on the Born-Oppenheimer approximation (see Chapter 3 for details) which assumes that coupling to nearby electronic states can be ignored. These assumptions are valid only when the energy surface of interest $E_j(R)$ is not crossed or closely approached by another electronic energy surface $E_k(R)$. When the electronic states are so widely spaced, it is proper to speak of the movement of the molecule(s) on the electronic surface $E_j(R)$, and to use either classical or quantum mechanical methods to follow such movements.

To simplify the notation throughout this Chapter, the above Schrödinger equation appropriate to movement on a single electronic energy surface will be written as follows:

$$[T + V(R)] \quad (R) = E \quad (R),$$

where T denotes the kinetic energy operator for <u>all</u> 3N of the geometrical coordinates (collectively denoted R) needed to specify the location of the N nuclei, V(R) is the electronic energy as a function of these coordinates, and
   (R) is the nuclear-motion wavefunction.

For example, when diatomic species are considered, V is a function of the radial coordinate describing the distance between the two nuclei, T contains derivatives with respect to radial as well as two angular coordinates (those pertaining to rotation or relative angular motion of the two nuclei), and R refers to these radial and angular coordinates. For a triatomic species such as H_2O, V is a function of two O-H bond lengths and the H-O-H angle, and R refers to these three internal coordinates as well as the three angle coordinates needed to specify the orientation of the H_2O molecule in space relative to a space-fixed

coordinate system (e.g., three Euler angles used in Chapter 3 to treat rotation of spherical and symmetric top molecules).

In Chapters 1 and 3 and in all of Section 4, such nuclear-motion Schrödinger equations were used to treat the <u>bound</u> vibrational motions of molecules (i.e., the movement of the nuclei when the energy available is not adequate to rupture one or more of the bonds in the molecule). These same Schrödinger equations also apply to the scattering of the constituent nuclei (e.g., the vibration-rotation motion of HCl is treated by the same Schrödinger equation as the scattering of an H atom and a Cl atom). The primary difference between these two situations lies in the total energy (E) available: in the former, E lies below the dissociation asymptote of the ground-state HCl electronic potential energy; in the latter E is higher than this asymptote (e.g., see the potential curve shown below with some of its bound state energies and a state in the continuum).
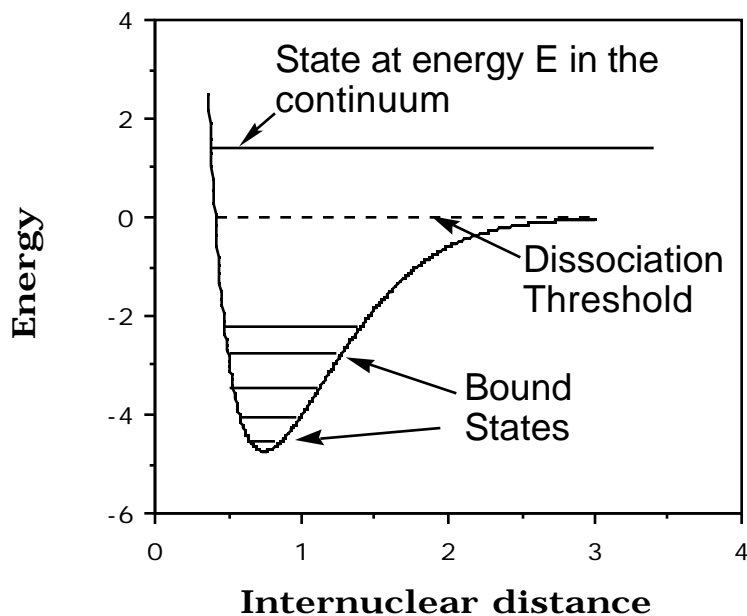
The different energies appropriate to bound-state and scattering situations affect the boundary conditions appropriate to the nuclear-motion wavefunctions in the large internuclear distance region. For the HCl example at hand, the bound-state vibrational wavefunctions $(R, \, ,)$ decay exponentially (see Chapter 1) for large R because such R-values lie in the classically forbidden region of R-space where E - V(R) is negative. In contrast, the scattering wavefunctions for this same V(R) potential and the same HCl molecule need not decay in the large-E region. As illustrated explicitly below for a model problem, this difference in large-R boundary conditions causes major differences in the eigenvalue spectrum of the Hamiltonian in these two cases. In particular, the bound-state

energy levels of HCl are discrete (i.e., quantized) but the scattering states are not (i.e., an H atom and a Cl atom may collide with arbitrary relative translational energy).

Let us now examine how the Schrödinger equation is solved for cases in which E lies above the dissociation energy of V(R) by considering a few simple model problems that can be solved exactly.

I. One Dimensional Scattering

Atom-atom scattering on a single Born-Oppenheimer energy surface can be reduced to a one-dimensional Schrödinger equation by separating the radial and angular parts of the three-dimensional Schrödinger equation in the same fashion as used for the Hydrogen atom in Chapter 1. The resultant equation for the radial part (R) of the wavefunction can be written as:

$$- (\hbar^2/2\mu) \, R^{-2} \, \partial/\partial R \, (R^2 \, \partial/\partial R) + L \, (L+1)\hbar^2/(2\mu R^2) + V(R) = E \, ,$$

where L is the quantum number that labels the angular momentum of the colliding particles whose reduced mass is μ.

Defining $\psi(R) = R \, \Psi(R)$ and substituting into the above equation gives the following equation for ψ:

$$- (\hbar^2/2\mu) \, \partial^2\psi/\partial R^2 + L \, (L+1)\hbar^2/(2\mu R^2)\psi + V(R)\psi = E\psi \, .$$

The combination of the "centrifugal potential" $L \, (L+1)\hbar^2/(2\mu R^2)$ and the electronic potential V(R) thus produce a total "effective potential" for describing the radial motion of the system.

The simplest reasonable model for such an effective potential is provided by the "square well" potential illustrated below. This model V(R) could, for example, be applied to the L = 0 scattering of two atoms whose bond dissociation energy is D_e and whose equilibrium bond length for this electronic surface lies somewhere between R = 0 and R = R_{max}.
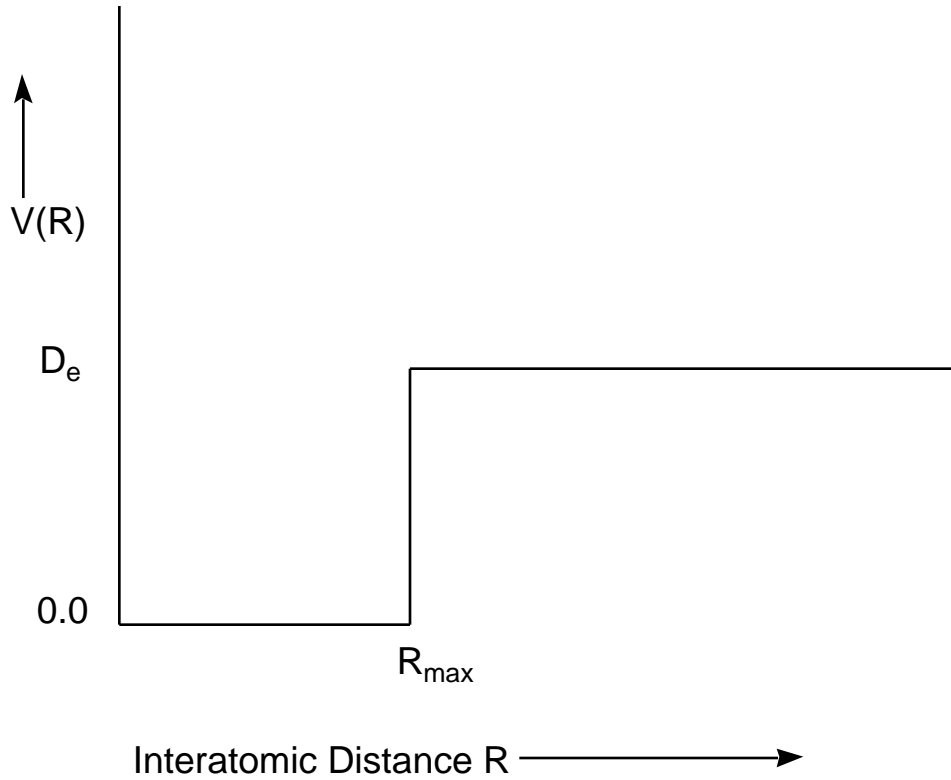
The piecewise constant nature of this particular V(R) allows exact solutions to be written both for bound and scattering states because the Schrödinger equation

$$- (\hbar^2/2\mu) \, d^2 \psi /dR^2 = E\psi \qquad (\text{for } 0 \le R \le R_{max})$$

$$- (\hbar^2/2\mu) \, d^2 \psi /dR^2 + D_e \psi = E\psi \qquad (R_{max} \le R < \infty)$$

admits simple sinusoidal solutions.

A. Bound States

The **bound states** are characterized by having $E < D_e$. For the inner region, the two solutions to the above equation are

$$\psi_1(R) = A \, \sin(kR)$$

and

$$\psi_2(R) = B \cos(kR)$$

where

$$k = \sqrt{2\mu E/\hbar^2}$$

is termed the "local wave number" because it is related to the momentum values for the $\exp(\pm i\,k\,R)$ components of such a function:

$$-i\hbar\ \partial\exp(\pm i\,k\,R)/\partial R = \hbar\,k\,\exp(\pm i\,k\,R).$$

The cos(kR) solution must be excluded (i.e., its amplitude B in the general solution of the Schrödinger equation must be chosen equal to 0.0) because this function does not vanish at $R = 0$, where the potential moves to infinity and thus the wavefunction must vanish. This means that only the

$$\psi = A \sin(kR)$$

term remains for this inner region.

Within the asymptotic region ($R > R_{max}$) there are also two solutions to the Schrödinger equation:

$$\psi_3 = C \exp(-\kappa R)$$

and

$$\psi_4 = D \exp(\kappa R)$$

where

$$\kappa = \sqrt{2\mu(D_e - E)/\hbar^2}\ \ .$$

Clearly, one of these functions is a decaying function of R for large R and the other ψ_4 grows exponentially for large R. The latter's amplitude D must be set to zero because this

function generates a probability density that grows larger and larger as R penetrates deeper and deeper into the classically forbidden region (where $E < V(R)$).

To connect ψ_1 in the inner region to ψ_3 in the outer region, we use the fact that ψ and $d\psi/dR$ must be continuous except at points R where $V(R)$ undergoes an infinite discontinuity (see Chapter 1). Continuity of ψ at R_{max} gives:

$$A \sin(kR_{max}) = C \exp(-\kappa R_{max}),$$

and continuity of $d\psi/dR$ at R_{max} yields

$$A k \cos(kR_{max}) = -\kappa C \exp(-\kappa R_{max}).$$

These two equations allow the ratio C/A as well as the energy E (which appears in κ and in k) to be determined:

$$A/C = -\kappa/k \exp(-\kappa R_{max})/\cos(kR_{max}).$$

The condition that determines E is based on the well known requirement that the determinant of coefficients must vanish for homogeneous linear equations to have no-trivial solutions (i.e., not $A = C = 0$):

$$\det \begin{vmatrix} \sin(kR_{max}) & -\exp(-\kappa R_{max}) \\ k\cos(kR_{max}) & \kappa\exp(-\kappa R_{max}) \end{vmatrix} = 0$$

The vanishing of this determinant can be rewritten as

$$\kappa \sin(kR_{max}) \exp(-\kappa R_{max}) + k \cos(kR_{max}) \exp(-\kappa R_{max}) = 0$$

or

$$\tan(kR_{max}) = -k/\kappa .$$

When employed in the expression for A/C, this result gives

$$A/C = \exp(-\kappa R_{max})/\sin(kR_{max}).$$

For very large D_e compared to E, the above equation for E reduces to the familiar "particle in a box" energy level result since $k/$ vanishes in this limit, and thus $\tan(kR_{max}) = 0$, which is equivalent to $\sin(kR_{max}) = 0$, which yields the familiar $E = n^2 h^2/(8\mu R^2_{max})$ and $C/A = 0$, so $= A \sin(kR)$.

When D_e is not large compared to E, the full transcendental equation $\tan(kR_{max}) = -k/$ must be solved numerically or graphically for the eigenvalues E_n, $n = 1, 2, 3, ...$. These energy levels, when substituted into the definitions for k and give the wavefunctions:

$$= A \sin(kR) \qquad (\text{for } 0 \quad R \quad R_{max})$$

$$= A \sin(kR_{max}) \exp(R_{max}) \exp(- R) \qquad (\text{for } R_{max} \quad R <).$$

The one remaining unknown A can be determined by requiring that the modulus squared of the wavefunction describe a probability density that is normalized to unity when integrated over all space:

$$\int_0 | |^2 \, dR = 1.$$

Note that this condition is equivalent to

$$\int_0 | |^2 R^2 dR = 1$$

which would pertain to the original radial wavefunction. In the case of an infinitely deep potential well, this normalization condition reduces to

$$\int_0^{R_{max}} A^2 \sin^2(kR) dR = 1$$

which produces

$$A = \sqrt{\frac{2}{R_{max}}} \quad .$$

B. Scattering States

The **scattering states** are treated in much the same manner. The functions ψ_1 and ψ_2 arise as above, and the amplitude of ψ_2 must again be chosen to vanish because ψ must vanish at R = 0 where the potential moves to infinity. However, in the exterior region (R > R_{max}), the two solutions are now written as:

$$\psi_3 = C \exp(ik'R)$$

$$\psi_4 = D \exp(-ik'R)$$

where the large-R local wavenumber

$$k' = \sqrt{2\mu(E - D_e)/\hbar^2}$$

arises because $E > D_e$ for scattering states.

The conditions that ψ and $d\psi/dR$ be continuous at R_{max} still apply:

$$A \sin(kR_{max}) = C \exp(i\,k'R_{max}) + D \exp(-i\,k'R_{max})$$

and

$$k\,A\,\cos(kR_{max}) = i\,k'C\,\exp(i\,k'R_{max}) - ik'\,D\,\exp(-i\,k'R_{max}).$$

However, these two equations (in <u>three</u> unknowns A, C, and D) can no longer be solved to generate eigenvalues E and amplitude ratios. There are now three amplitudes as well as the E value but only these two equations plus a normalization condition to be used. The result is that the energy no longer is specified by a boundary condition; it can take on any value. We thus speak of scattering states as being "in the continuum" because the allowed values of E form a continuum beginning at $E = D_e$ (since the zero of energy is defined in this example as at the bottom of the potential well).

The R > R_{max} components of ψ are commonly referred to as "incoming"

$$\psi_{in} = D \exp(-ik'R)$$

and "outgoing"

$$\psi_{out} = C \exp(ik'R)$$

because their radial momentum eigenvalues are $-\hbar k'$ and $\hbar k'$, respectively. It is a common convention to define the amplitude D so that the **flux** of incoming particles is unity. Choosing

$$D = \sqrt{\frac{\mu}{\hbar k'}}$$

produces an incoming wavefunction whose current density is:

$$S(R) = -i\hbar/2\mu \ [\ \psi_{in}^* \ (d/dR \ \psi_{in}) - (d \ \psi_{in}/dR)^* \ \psi_{in}]$$

$$= |D|^2 \ (-i\hbar/2\mu) \ [-2ik']$$

$$= -1.$$

This means that there is one unit of current density moving inward (this produces the minus sign) for all values of R at which ψ_{in} is an appropriate wavefunction (i.e., $R > R_{max}$). This condition takes the place of the probability normalization condition specified in the bound-state case when the modulus squared of the total wavefunction is required to be normalized to unity over all space. Scattering wavefunctions can not be so normalized because they do not decay at large R; for this reason, the flux normalization condition is usually employed. The magnitudes of the outgoing (C) and short range (A) wavefunctions relative to that of the incoming function (D) then provide information about the scattering and "trapping" of incident flux by the interaction potential.

Once D is so specified, the above two boundary matching equations are written as a set of two inhomogeneous linear equations in two unknowns (A and C):

$$A \sin(kR_{max}) - C \exp(i \ k'R_{max}) = D \exp(-i \ k'R_{max})$$

and

$$k\, A \cos(kR_{max}) - i\, k'C \exp(i\, k'R_{max}) = -\, ik'\, D \exp(-i\, k'R_{max})$$

or

$$\begin{pmatrix} \sin(kR_{max}) & -\exp(i\, k'R_{max}) \\ k\cos(kR_{max}) & -i\, k'\exp(i\, k'R_{max}) \end{pmatrix} \begin{pmatrix} A \\ C \end{pmatrix} = \begin{pmatrix} D \exp(-i\, k'R_{max}) \\ -\, ik'\, D \exp(-i\, k'R_{max}) \end{pmatrix} .$$

Non-trivial solutions for A and C will exist except when the determinant of the matrix on the left side vanishes:

$$-i\, k' \sin(kR_{max}) + k \cos(kR_{max}) = 0,$$

which can be true only if

$$\tan(kR_{max}) = ik'/k.$$

This equation is not obeyed for any (real) value of the energy E, so solutions for A and C in terms of the specified D can always be found.

In summary, specification of unit incident flux is made by choosing D as indicated above. For any collision energy $E > D_e$, the 2x1 array on the right hand side of the set of linear equations written above can be formed, as can the 2x2 matrix on the left side. These linear equations can then be solved for A and C. The overall wavefunction for this E is then given by:

$$= A \sin(kR) \qquad\qquad (\text{for } 0 \le R \le R_{max})$$

$$= C \exp(ik'R) + D \exp(-ik'R) \qquad (\text{for } R_{max} \le R < \infty).$$

C. Shape Resonance States

If the angular momentum quantum number L in the effective potential introduced earlier is non-zero, this potential has a repulsive component at large R. This repulsion can combine with short-range attractive interactions due, for example, to chemical bond forces,

to produce an effective potential that one can model in terms of simple piecewise functions shown below.
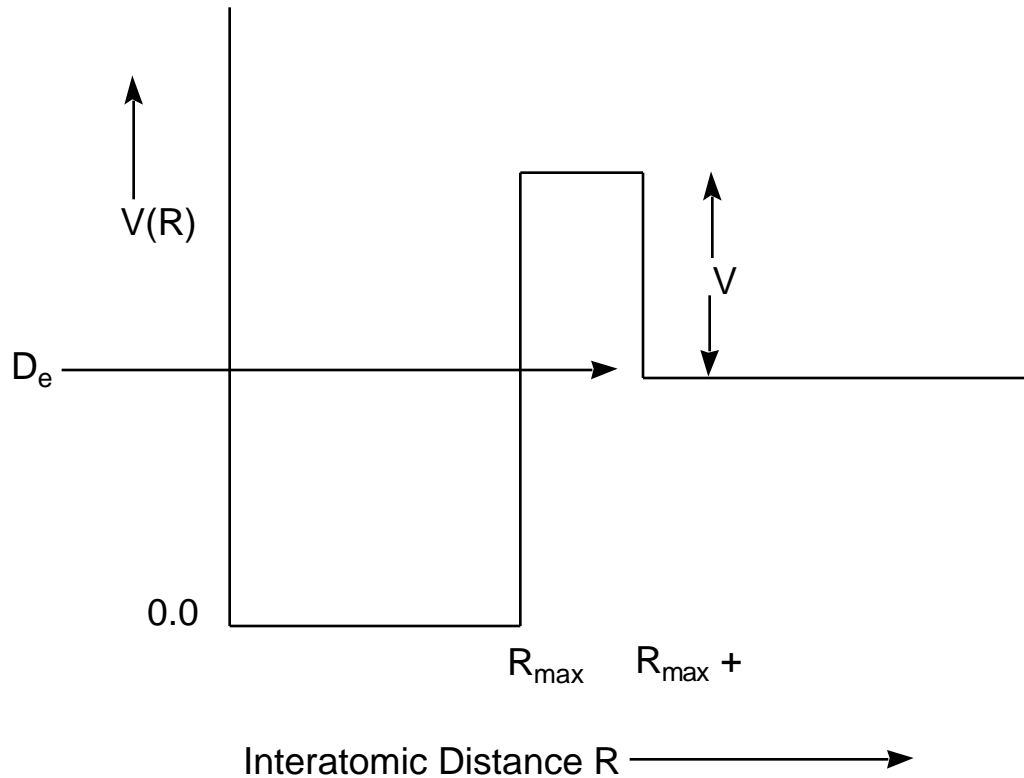
Again, the piecewise nature of the potential allows the one-dimensional Schrödinger equation to be solved analytically. For energies below D_e, one again finds bound states in much the same way as illustrated above (but with the exponentially decaying function exp(- 'R) used in the region R_{max} R $R_{max} + $, with $' = \sqrt{2\mu(D_e + V - E)/\hbar^2}$).

For energies lying above $D_e + V$, scattering states occur and the four amplitudes of the functions (sin(kR), exp($\pm$i k'''R) with $k''' = \sqrt{2\mu(-D_e - V + E)/\hbar^2}$, and exp(i k'R)) appropriate to each R-region are determined in terms of the amplitude of the incoming asymptotic function D exp(-ik'R) from the four equations obtained by matching and d /dR at R_{max} and at $R_{max} + $.

For energies lying in the range $D_e < E < D_e + V$, a qualitatively different class of scattering function exists. These so-called **shape resonance** states occur at energies that are determined by the condition that the amplitude of the wavefunction within the barrier (i.e., for 0 R R_{max}) be large so that incident flux successfully tunnels through the

barrier and builds up, through constructive interference, large probability amplitude there. Let us now turn our attention to this specific energy regime.

The piecewise solutions to the Schrödinger equation appropriate to the shape-resonance case are easily written down:

$$\psi = A\sin(kR) \qquad\qquad \text{(for } 0 \le R \le R_{max})$$

$$\psi = B_+ \exp(\kappa'R) + B_- \exp(-\kappa'R) \qquad \text{(for } R_{max} \le R \le R_{max} + \delta)$$

$$\psi = C \exp(ik'R) + D \exp(-ik'R) \qquad \text{(for } R_{max} + \delta \le R < \infty).$$

Note that both exponentially growing and decaying functions are acceptable in the $R_{max} \le R \le R_{max} + \delta$ region because this region does not extend to $R = \infty$. There are four amplitudes (A, B_+, B_-, and C) that must be expressed in terms of the specified amplitude D of the incoming flux. Four equations that can be used to achieve this goal result when ψ and $d\psi/dR$ are matched at R_{max} and at $R_{max} + \delta$:

$$A\sin(kR_{max}) = B_+ \exp(\kappa'R_{max}) + B_- \exp(-\kappa'R_{max}),$$

$$Ak\cos(kR_{max}) = \kappa'B_+ \exp(\kappa'R_{max}) - \kappa'B_- \exp(-\kappa'R_{max}),$$

$$B_+ \exp(\kappa'(R_{max} + \delta)) + B_- \exp(-\kappa'(R_{max} + \delta))$$

$$= C \exp(ik'(R_{max} + \delta)) + D \exp(-ik'(R_{max} + \delta)),$$

$$\kappa'B_+ \exp(\kappa'(R_{max} + \delta)) - \kappa'B_- \exp(-\kappa'(R_{max} + \delta))$$

$$= ik'C \exp(ik'(R_{max} + \delta)) - ik' D \exp(-ik'(R_{max} + \delta)).$$

It is especially instructive to consider the value of A/D that results from solving this set of four equations in four unknowns because the modulus of this ratio provides information about the relative amount of amplitude that exists inside the centrifugal barrier in the attractive region of the potential compared to that existing in the asymptotic region as incoming flux.

The result of solving for A/D is:

$$A/D = 4 \quad \text{'exp(-ik'}(R_{max}+\ ))$$

$$\{\exp(\ '\ )(ik'-\ ')(\ '\sin(kR_{max})+k\cos(kR_{max}))/ik'$$

$$+ \exp(-\ '\ )(ik'+\ ')(\ '\sin(kR_{max})-k\cos(kR_{max}))/ik'\ \}^{-1}.$$

Further, it is instructive to consider this result under conditions of a high (large $D_e +\ V -$ E) and thick (large) barrier. In such a case, the "tunnelling factor" $\exp(-\ '\ )$ will be very small compared to its counterpart $\exp(\ '\ )$, and so

$$A/D = 4\ \frac{ik'\ '}{ik'-\ '}\ \exp(-ik'(R_{max}+\ ))\ \exp(-\ '\ )\ \{\ '\sin(kR_{max})+k\cos(kR_{max})\ \}^{-1}.$$

The $\exp(-\ '\ )$ factor in A/D causes the magnitude of the wavefunction inside the barrier to be small in most circumstances; we say that incident flux must tunnel through the barrier to reach the inner region and that $\exp(-\ '\ )$ gives the probability of this tunnelling. The magnitude of the A/D factor could become large if the collision energy E is such that

$$'\sin(kR_{max})+k\cos(kR_{max})$$

is small. In fact, if

$$\tan(kR_{max}) = -\ k/\ '$$

this denominator factor in A/D will vanish and A/D will become infinite. Note that the above condition is similar to the energy quantization condition

$$\tan(kR_{max}) = -\ k/$$

that arose when bound states of a finite potential well were examined earlier in this Chapter. There is, however, an important difference. In the bound-state situation

$$k = \sqrt{2\mu E/\hbar^2}$$

and

$$\kappa = \sqrt{2\mu(D_e - E)/\hbar^2} \; ;$$

in this shape-resonance case, k is the same, but

$$\kappa' = \sqrt{2\mu(D_e + V - E)/\hbar^2} \,)$$

rather than κ occurs, so the two $\tan(kR_{max})$ equations are not identical.
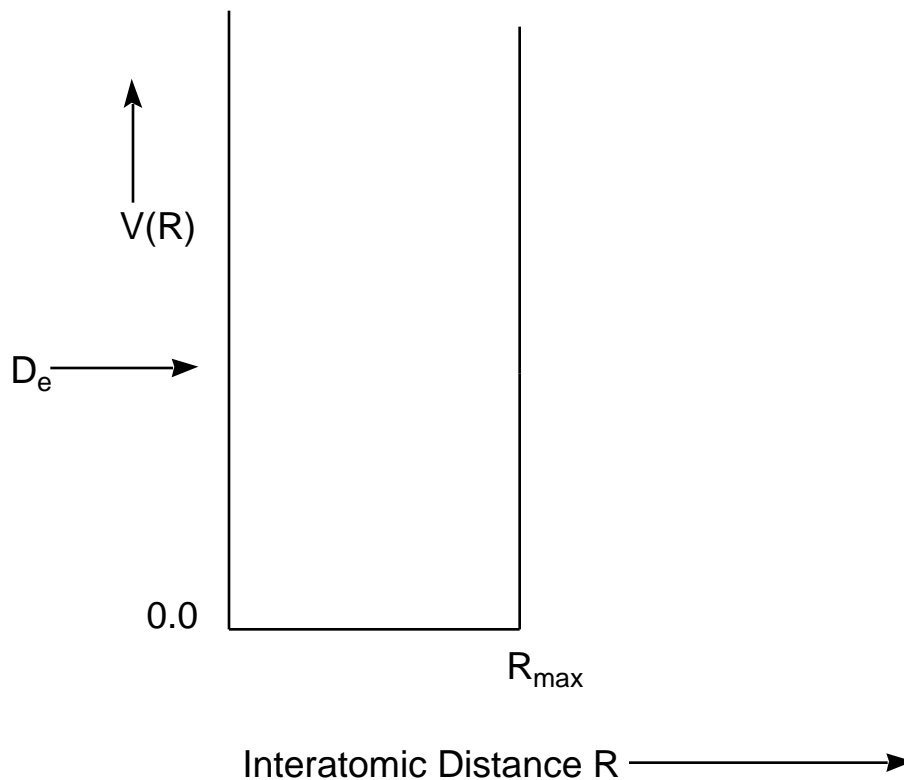
However, in the case of a very high barrier (so that κ' is much larger than k), the denominator

$$\kappa'\sin(kR_{max}) + k\cos(kR_{max}) \approx \kappa' \sin(kR_{max})$$

in A/D can become small if

$$\sin(kR_{max}) \approx 0.$$

This condition is nothing but the energy quantization condition that would occur for the particle-in-a-box potential shown below.

This potential is identical to the true effective potential for $0 \leq R \leq R_{max}$, but extends to infinity beyond R_{max}; the barrier and the dissociation asymptote displayed by the true potential are absent.

In summary, when a barrier is present on a potential energy surface, at energies above the dissociation asymptote D_e but below the top of the barrier ($D_e + \Delta V$ here), one can expect shape-resonance states to occur at "special" scattering energies E. These so-called resonance energies can often be approximated by the bound-state energies of a potential that is identical to the potential of interest in the inner region ($0 \leq R \leq R_{max}$ here) but that extends to infinity beyond the top of the barrier (i.e., beyond the barrier, it does not fall back to values below E).

The chemical significance of shape resonances is great. Highly rotationally excited molecules may have more than enough total energy to dissociate (D_e), but this energy may be "stored" in the rotational motion, and the vibrational energy may be less than D_e. In terms of the above model, high angular momentum may produce a significant barrier in the effective potential, but the system's vibrational energy may lie significantly below D_e. In such a case, and when viewed in terms of motion on an angular momentum modified effective potential, the lifetime of the molecule with respect to dissociation is determined by the rate of tunnelling through the barrier.

For the case at hand, one speaks of "rotational predissociation" of the molecule. The lifetime   can be estimated by computing the frequency   at which flux existing inside R_{max} strikes the barrier at R_{max}

$$= \frac{\hbar k}{2\mu R_{max}} \quad (sec^{-1})$$

and then multiplying by the probability P that flux tunnels through the barrier from R_{max} to $R_{max} +$:

$$P = \exp(-2 \ ' \ ).$$

The result is that

$$^{-1} = \frac{\hbar k}{2\mu R_{max}} \ \exp(-2 \ ' \ )$$

with the energy E entering into k and   ' being determined by the resonance condition:
('sin(kR_{max})+kcos(kR_{max})) = minimum.

Although the examples treated above involved piecewise constant potentials (so the Schrödinger equation and the boundary matching conditions could be solved exactly), many of the characteristics observed carry over to more chemically realistic situations. As discussed, for example, in Energetic Principles of Chemical Reactions, *J. Simons, Jones and Bartlett, Portola Valley, Calif. (1983), one can often model chemical reaction processes in terms of:*

(i) motion along a "reaction coordinate" (s) from a region characteristic of reactant materials where the potential surface is positively curved in all direction and all forces (i.e., gradients of the potential along all internal coordinates) vanish,

(ii) to a transition state at which the potential surface's curvature along s is negative while all other curvatures are positive and all forces vanish,

(iii) onward to product materials where again all curvatures are positive and all forces vanish.

Within such a "reaction path" point of view, motion transverse to the reaction coordinate s is often modelled in terms of local harmonic motion although more sophisticated treatments of the dynamics is possible. In any event, this picture leads one to consider motion along a single degree of freedom (s), with respect to which much of the above treatment can be carried over, coupled to transverse motion along all other internal degrees of freedom taking place under an entirely positively curved potential (which therefore produces restoring forces to movement away from the "streambed" traced out by the reaction path s).

II. Multichannel Problems

When excited electronic states are involved, couplings between two or more electronic surfaces may arise. Dynamics occuring on an excited-state surface may evolve in a way that produces flux on another surface. For example, collisions between an electronically excited 1s2s (^{3}S) He atom and a ground-state 1s^2 (^{1}S) He atom occur on a potential energy surface that is repulsive at large R (due to the repulsive interaction between the closed-shell 1s^2 He and the large 2s orbital) but attractive at smaller R (due to the $\sigma^2 \sigma^{*1}$ orbital occupancy arising from the three 1s-derived electrons). The ground-state potential energy surface for this system (pertaining to two 1s^2 (^{1}S) He atoms is repulsive at small R values (because of the $\sigma^2 \sigma^{*2}$ nature of the electronic state). In this case, there are two Born-Oppenheimer electronic-nuclear motion states that are degenerate and thus need to be combined to achieve a proper description of the dynamics:

$$\Psi_1 = |\sigma^2 \sigma^{*2}|\ \chi_{grnd.}(R, \theta, \phi)$$

pertaining to the ground electronic state and the scattering state $\chi_{grnd.}$ on this energy surface, and

$$\Psi_2 = |\sigma^2 \sigma^{*1}2\sigma^1|\ \chi_{ex.}(R, \theta, \phi)$$

pertaining to the excited electronic state and the nuclear-motion state $\chi_{ex.}$ on this energy surface. Both of these wavefunctions can have the same energy E; the former has high nuclear-motion energy and low electronic energy, while the latter has higher electronic energy and lower nuclear-motion energy.

A simple model that can be used to illustrate the two-state couplings that arise in such cases is introduced through the two one-dimensional piecewise potential surfaces shown below.
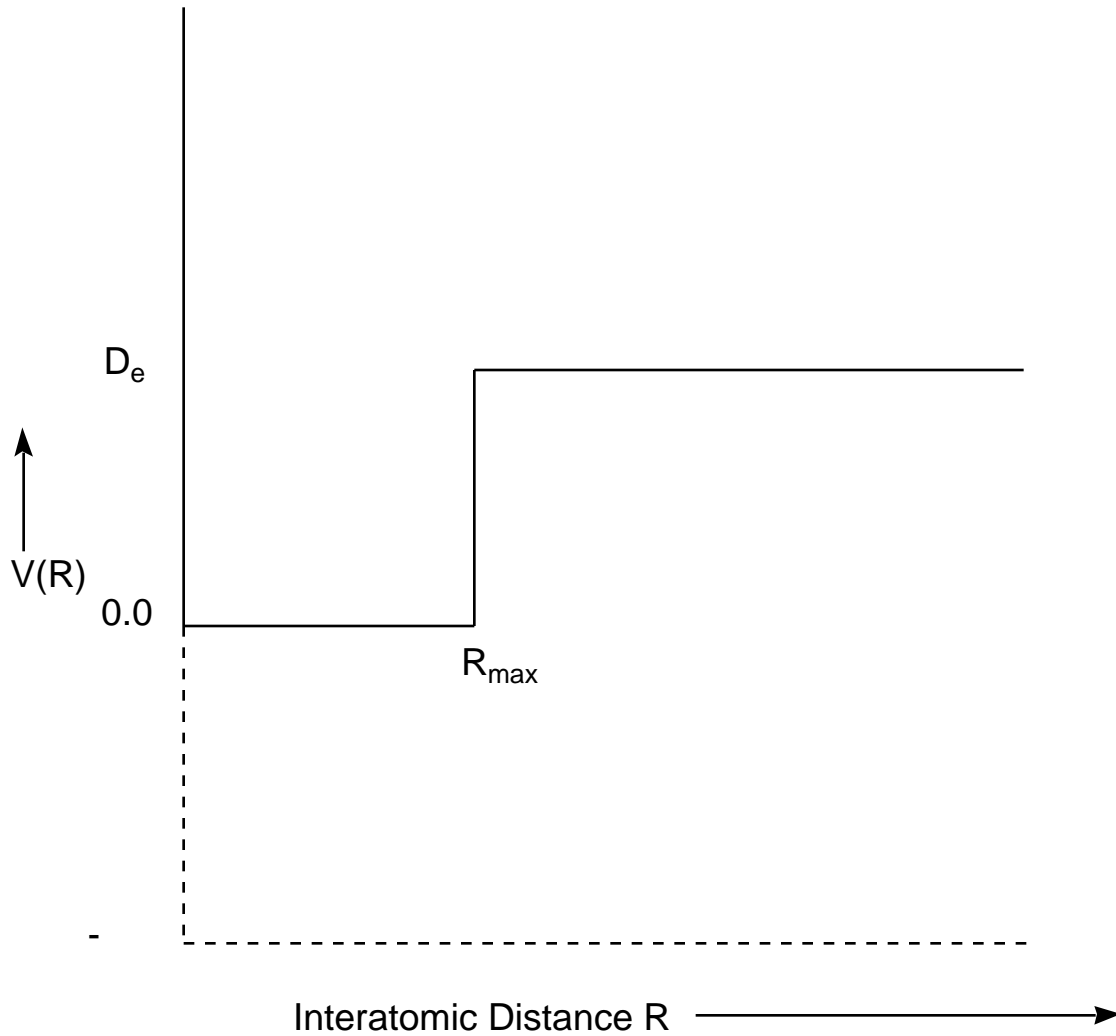
The dashed energy surface

$$V(R) = - \qquad \text{(for } 0 \quad R < \quad)$$

provides a simple representation of a repulsive lower-energy surface, and the solid-line plot represents the excited-state surface that has a well of depth D_e and whose well lies   above the ground-state surface.

In this case, and for energies lying above zero (for $E < 0$, only nuclear motion on the lower energy dashed surface is "open" (i.e., accessible)) yet below D_e, the nuclear-

motion wavefunction can have amplitudes belonging to both surfaces. That is, the total (electronic and nuclear) wavefunction consists of two portions that can be written as:

$$= A \; \sin(kR) + \; '' A'' \sin(k''R) \qquad (\text{for } 0 \quad R \quad R_{max})$$

and

$$= A \; \sin(kR_{max}) \exp(\; R_{max}) \exp(- \; R) + \; '' A'' \sin(k''R)$$

$$(\text{for } R_{max} \quad R < \quad),$$

where and " denote the electronic functions belonging to the upper and lower energy surfaces, respectively. The wavenumbers k and k" are defined as:

$$k = \sqrt{2\mu E/\hbar^2}$$

$$k'' = \sqrt{2\mu(E + \quad)/\hbar^2}$$

and is as before

$$= \sqrt{2\mu(D_e - E)/\hbar^2} \; .$$

For the lower-energy surface, only the sin(k"R) function is allowed because the cos(k"R) function does not vanish at R = 0.

A. The Coupled Channel Equations

In such cases, the relative amplitudes (A and A") of the nuclear motion wavefunctions on each surface must be determined by substituting the above "two-channel" wavefunction (the word channel is used to denote separate asymptotic states of the system; in this case, the and " electronic states) into the full Schrödinger equation. In Chapter 3,

the couplings among Born-Oppenheimer states were so treated and resulted in the following equation:

$$[(E_j(R) - E) \chi_j(R) + T \chi_j(R)] = - \sum_i \{ < \psi_j | T | \psi_i > (R) \chi_i(R)$$

$$+ \sum_{a=1,M} (- \hbar^2/m_a) < \psi_j | \nabla_a | \psi_i > (R) \cdot \nabla_a \chi_i(R) \}$$

where $E_j(R)$ and $\chi_j(R)$ denote the electronic energy surfaces and nuclear-motion wavefunctions, ψ_j denote the corresponding electronic wavefunctions, and the ∇_a represent derivatives with respect to the various coordinates of the nuclei.   Changing to the notation used in the one-dimensional model problem introduced above, these so-called **coupled-channel** equations read:

$$[(-\varepsilon - E) - \hbar^2/2\mu \, d^2/dR^2] \, A''\sin(k''R)$$

$$= - \{< \psi''| - \hbar^2/2\mu \, d^2/dR^2| \psi''> A''\sin(k''R)$$

$$+ (- \hbar^2/\mu) < \psi''|d/dR| \psi'> d/dR \, A \sin(kR) \} \qquad \text{(for } 0 \le R \le R_{max}),$$

$$[(-\varepsilon - E) - \hbar^2/2\mu \, d^2/dR^2] \, A''\sin(k''R)$$

$$= - \{< \psi''| - \hbar^2/2\mu \, d^2/dR^2| \psi''> A''\sin(k''R)$$

$$+ (- \hbar^2/\mu) < \psi''|d/dR| \psi'> d/dR \, A \sin(kR_{max}) \exp(\kappa R_{max}) \exp(- \kappa R) \}$$

$$\text{(for } R_{max} \le R < \infty);$$

when the index j refers to the ground-state surface $(V(R) = -\varepsilon$, for $0 < R < \infty)$, and

$$[(0 - E) - \hbar^2/2\mu \, d^2/dR^2] \, A\sin(kR) = - \{< \psi | - \hbar^2/2\mu \, d^2/dR^2| \psi > A\sin(kR)$$

$$+ (- \hbar^2/\mu) < \psi|d/dR| \psi''> d/dR \, A'' \sin(k''R) \} \text{(for } 0 \le R \le R_{max}),$$

$$[(D_e - E) - \hbar^2/2\mu \, d^2/dR^2] \, A\sin(kR_{max}) \exp(\kappa R_{max}) \exp(- \kappa R)$$

$$= - \{ < \quad |- \hbar^2/2\mu \ d^2/dR^2| \quad > A\sin(kR_{max}) \exp(\quad R_{max}) \exp(- \quad R)$$

$$+ (\ - \hbar^2/\mu) < \quad |d/dR| \quad "> d/dR \ A"\sin(k"R) \ \} \quad (\text{for } R_{max} \quad R < \quad)$$

when the index j refers to the excited-state surface (where $V(R) = 0$, for $0 < R \quad R_{max}$ and $V(R) = D_e$ for $R_{max} \quad R < \quad $).

Clearly, if the right-hand sides of the above equations are ignored, one simply recaptures the Schrödinger equations describing motion on the separate potential energy surfaces:

$$[(- \quad - E) - \hbar^2/2\mu \ d^2/dR^2 \ ] \ A"\sin(k"R) = 0 \qquad (\text{for } 0 \quad R \quad R_{max}),$$

$$[(- \quad - E) - \hbar^2/2\mu \ d^2/dR^2 \ ] \ A"\sin(k"R) = 0 \qquad (\text{for } R_{max} \quad R < \quad);$$

that describe motion on the lower-energy surface, and

$$[(0 - E) - \hbar^2/2\mu \ d^2/dR^2 \ ] \ A\sin(kR) = 0 \qquad (\text{for } 0 \quad R \quad R_{max}),$$

$$[(D_e - E) - \hbar^2/2\mu \ d^2/dR^2 \ ] \ A\sin(kR_{max}) \exp(\quad R_{max}) \exp(- \quad R) = 0$$

$$(\text{for } R_{max} \quad R < \quad)$$

describing motion on the upper surface on which the bonding interaction occurs. The terms on the right-hand sides provide the couplings that cause the true solutions to the Schrödinger equation to be combinations of solutions for the two separate surfaces.

In applications of the coupled-channel approach illustrated above, coupled sets of second order differential equations (two in the above example) are solved by starting with a specified flux in one of the channels and a chosen energy E. For example, one might specify the amplitude A to be unity to represent preparation of the system in a bound vibrational level (with $E < D_e$) of the excited electronic-state potential. One would then choose E to be one of the eigenenergies of that potential. Propagation methods could be used to solve the coupled differential equations subject to these choices of E and A. The

result would be the determination of the amplitude A' of the wavefunction on the ground-state surface. The ratio A'/A provides a measure of the strength of coupling between the two Born-Oppenheimer states.

B. Perturbative Treatment

Alternatively, one can treat the coupling between the two states via time dependent perturbation theory. For example, by taking A = 1.0 and choosing E to be one of the eigenenergies of the excited-state potential, one is specifying that the system is initially (just prior to t = 0) prepared in a state whose wavefunction is:

$$\Psi^0_{ex} = \quad \sin(kR) \hspace{4cm} (\text{for } 0 \leq R \leq R_{max})$$

$$\Psi^0_{ex} = \quad \sin(kR_{max}) \exp(\kappa R_{max}) \exp(-\kappa R) \quad (\text{for } R_{max} \leq R < \infty).$$

From t = 0 on, the coupling to the other state

$$\Psi^0_{grnd} = \quad \Psi' \sin(k'R) \hspace{4cm} (\text{for } 0 \leq R < \infty)$$

is induced by the "perturbation" embodied in the terms on the right-hand side of the coupled-channel equations.

Within this time dependent perturbation theory framework, the rate of transition of probability amplitude from the initially prepared state (on the excited state surface) to the ground-state surface is proportional to the square of the perturbation matrix elements between these two states:

$$\text{Rate} \approx | \int_0^{R_{max}} \sin(kR) < \Psi | d/dR | \Psi'' > (d/dR \sin(k''R)) dR$$

$$+ \int_{R_{max}}^{\infty} \sin(kR_{max}) \exp(\kappa R_{max}) \exp(-\kappa R) < \Psi | d/dR | \Psi'' > (d/dR \sin(k''R)) dR |^2$$

The matrix elements occurring here contain two distinct parts:

$$< \ |d/dR| \ ''>$$

has to do with the electronic state couplings that are induced by radial movement of the nuclei; and both

$$\sin(kR) \ d/dR\sin(k''R)$$

and

$$\sin(kR_{max}) \ \exp(\ R_{max}) \ \exp(- \ R) \ d/dR \ \sin(k''R)$$

relate to couplings between the two nuclear-motion wavefunctions induced by these same radial motions. For a transition to occur, both the electronic and nuclear-motion states must undergo changes. The initially prepared state (the bound state on the upper electronic surface) has high electronic and low nuclear-motion energy, while the state to which transitions may occur (the scattering state on the lower electronic surface) has low electronic energy and higher nuclear-motion energy.

Of course, in the above example, the integrals over R can be carried out if the electronic matrix elements $< \ |d/dR| \ ''>$ can be handled. In practical chemical applications (for an introductory treatment see Energetic Principles of Chemical Reactions, J. Simons, Jones and Bartlett, Portola Valley, Calif. (1983)), the evaluation of these electronic matrix elements is a formidable task that often requires computation intensive techniques such as those discussed in Section 6.

Even when the electronic coupling elements are available (or are modelled or parameterized in some reasonable manner), the solution of the coupled-channel equations that govern the nuclear motion is a demanding task. For the purposes of this text, it suffices to note that:

(i) couplings between motion on two or more electronic states can and do occur;

(ii) these couplings are essential to treat whenever the electronic energy difference (i.e., the spacing between pairs of Born-Oppenheimer potential surfaces) is small (i.e., comparable to vibrational or rotational energy level spacings);

(iii) there exists a rigorous theoretical framework in terms of which one can evaluate the rates of so-called **radiationless transitions** between pairs of such electronic,

vibrational, rotational states. Expressions for such transitions involve (a) electronic matrix elements < |d/dR| "> that depend on how strongly the electronic states are modulated by movement (hence the d/dR) of the nuclei, and (b) nuclear-motion integrals connecting the initial and final nuclear-motion wavefunctions, which also contain d/dR because they describe the "recoil" of the nuclei induced by the electronic transition.

C. Chemical Relevance

As presented above, the most obvious situation of multichannel dynamics arises when electronically excited molecules undergo radiationless relaxation (e.g., internal conversion when the spin symmetry of the two states is the same or intersystem crossing when the two states differ in spin symmetry). These subjects are treated in some detail in the text Energetic Principles of Chemical Reactions, J. Simons, Jones and Bartlett, Portola Valley, Calif. (1983)) where radiationless transitions arising in photochemistry and polyatomic molecule reactivity are discussed.

Let us consider an example involving the chemical reactivity of electronically excited alkaline earth or $d^{10}s^2$ transition metal atoms with H_2 molecules. The particular case for $Cd^* + H_2 \quad CdH + H$ has been studied experimentally and theoretically. In such systems, the potential energy surface connecting to ground-state Cd (^1S) + H_2 becomes highly repulsive as the collision partners approach (see the depiction provided in the Figure shown below). The three surfaces that correlate with the Cd (^1P) + H_2 species prepared by photo-excitation of Cd (^1S) behave quite differently as functions of the Cd-to-H_2 distance because in each the singly occupied 6p orbital assumes a different orientation relative to the H_2 molecule's bond axis. For (near) C_{2v} orientations, these states are labeled $^1B_2$, $^1B_1$, and $^1A_1$; they have the 6p orbital directed as shown in the second Figure, respectively. The corresponding triplet surfaces that derive from Cd (^3P) + H_2 behave, as functions of the Cd-to-H_2 distance (R) in similar manner, except they are shifted to lower energy because Cd (^3P) lies below Cd (^1P) by ca. 37 kcal/mol.

Collisions between Cd (^1P) and H_2 can occur on any of the three surfaces mentioned above. Flus on the $^1A_1$ surface is primarily reflected (at low collision energies characteristic of the thermal experiments) because this surface is quite repulsive at large R. Flux on the $^1B_1$ surface can proceed in to quite small R (ca. 2.4 Å) before repulsive forces on this surface reflect it. At geometries near R = 2.0Å and r_{HH} = 0.88 Å, the highly repulsive $^3A_1$ surface intersects this $^1B_1$ surface from below. At and near this intersection, a combination of spin-orbit coupling (which is large for Cd) and non-adiabatic coupling

may induce flux to evolve onto the $^3A_1$ surface, after which fragmentation to Cd $(^3P) + H_2$ could occur.

In contrast, flux on the $^1B_2$ surface propogates inward under attractive forces to R = 2.25 Å and r_{HH} = 0.79 Å where it may evolve onto the $^3A_1$ surface which intersects from below. At and near this intersection, a combination of spin-orbit coupling (which is large for Cd) and non-adiabatic coupling may induce flux to evolve onto the $^3A_1$ surface, after which fragmentation to Cd $(^3P) + H_2$ could occur. Flux that continues to propogate inward to smaller R values experiences even stronger attractive forces that lead, near R = 1.69 Å and r_{HH} = 1.54 Å, to an intersection with the $^1A_1$ surface that connects to Cd $(^1S) + H_2$. Here, non-adiabatic couplings may cause flux to evolve onto the $^1A_1$ surface which may then lead to formation of ground state Cd $(^1S) + H_2$ or Cd $(^1S) + H + H$, both of which are energetically possible. Processes in which electronically excited atoms produce ground-state atoms through such collisions and surface hopping are termed "electronic quenching".

The nature of the non-adiabatic couplings that arise in the two examples given above are quite different. In the former case, when the $^1B_1$ and $^3A_1$ surfaces are in close proximity to one another, the first-order coupling element:

$$< \psi(^1B_1) | \frac{\partial}{\partial Q_j} | \psi(^3A_1)>$$

is non-zero only for nuclear motions (i.e., Q_j) of $b_1 \times a_1 = b_1$ symmetry. For the CdH$_2$ collision complex being considered in (or near) C_{2v} symmetry, such a motion corresponds to rotational motion of the nuclei about an axis lying parallel to the H-H bond axis. In contrast, to couple the $^3A_1$ and $^1B_2$ electronic states through an element of the form

$$< \psi(^1B_2) | \frac{\partial}{\partial Q_j} | \psi(^3A_1)>,$$

the motion must be of $b_2 \times a_1 = b_2$ symmetry. This movement corresponds to asymmetric vibrational motion of the two Cd-H interatomic coordinates.

The implications of these observations are clear. For example, in so-called half-collision experiments in which a van der Waals CdH$_2$ complex is probed, internal rotational motion would be expected to enhance $^1B_1 \rightarrow {}^3A_1$ quenching, whereas asymmetric vibrational motion should enhance the $^1B_2 \rightarrow {}^3A_1$ process.
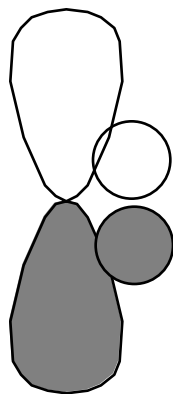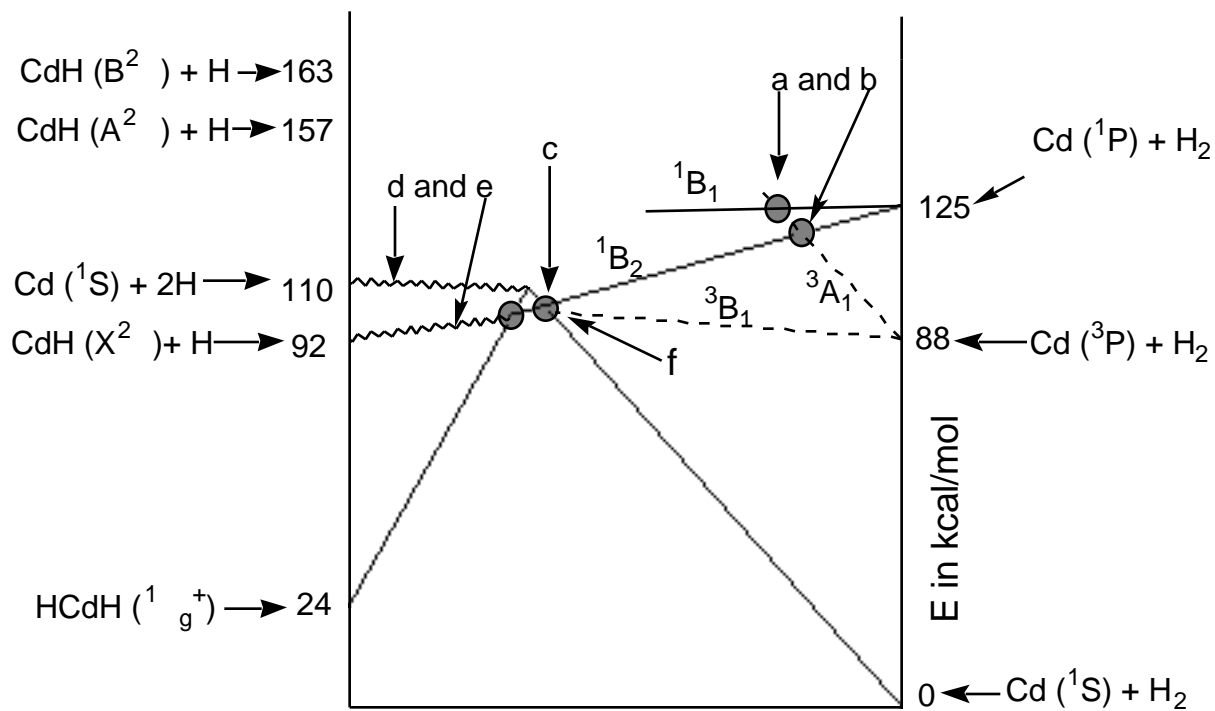
Moreover, the production of ground-state Cd $(^1S) + H_2$ via $^1B_2 \rightarrow {}^1A_1$ surface hopping (near R = 1.69 Å and r_{HH} = 1.54 Å) should also be enhanced by asymmetric vibrational excitation. The $^1B_2$ and $^1A_1$ surfaces also provide, through their non-adiabatic couplings, a "gateway" to formation of the asymmetric bond cleavage products CdH $(^2\Sigma)$ +

H. It can be shown that the curvature (i.e., second energy derivative) of a potential energy surface consists of two parts: (i) one part that in always positive, and (ii) a second that can be represented in terms of the non-adiabatic coupling elements between the two surfaces and the energy gap ΔE between the two surfaces. Applied to the two states at hand, this second contributor to the curvature of the $^1B_2$ surface is:
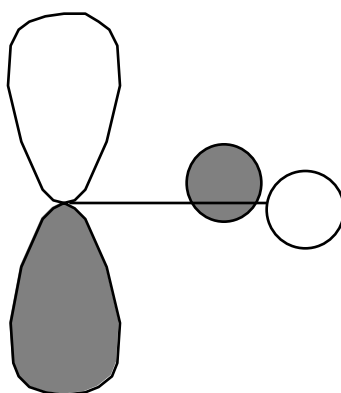
$$\frac{|<\psi(^1B_2)\,|\,\frac{\partial}{\partial q_j}\,|\,\psi(^1A_1)>\,|^2}{E(^1B_2)\,-\,E(^1A_1)}\,.$$

Clearly, when the $^1A_1$ state is higher in energy but strongly non-adiabatically coupled to the $^1B_2$ state, negative curvature along the asymmetric b_2 vibrational mode is expected for the $^1B_2$ state. When the $^1A_1$ state is lower in energy, negative curvature along the b_2 vibrational mode is expected for the $^1A_1$ state (because the above expression also expresses the curvature of the $^1A_1$ state).

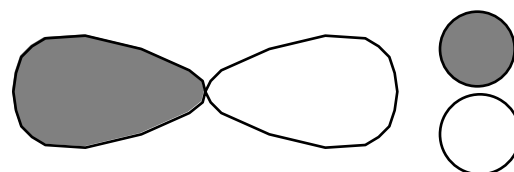   Therefore, in the region of close-approach of these two states, state-to-state surface hopping can be facile. Moreover, one of the two states (the lower lying at each geometry) will likely possess negative curvature along the b_2 vibrational mode. It is this negative curvature that causes movement away from C_{2v} symmetry to occur spontaneously, thus leading to the CdH ($^2\Sigma$) + H reaction products.

CdH (B^2) + H → 163

CdH (A^2) + H → 157

d and e

c

a and b

$^1B_1$

Cd (^1P) + H_2

125

Cd (^1S) + 2H → 110

$^1B_2$

$^3A_1$

CdH (X^2)+ H → 92

$^3B_1$

f

88 ← Cd (^3P) + H_2

E in kcal/mol

HCdH ($^1\Sigma_g^+$) → 24

0 ← Cd (^1S) + H_2

b₂ overlap
of Cd 6p orbital
and H₂ σg orbital

b₁ overlap
of Cd 6p orbital
and H₂ σg orbital

a₁ overlap
of Cd 6p orbital
and H₂ σg orbital

Coupled-state dynamics can also be used to describe situations in which vibrational rather than electronic-state transitions occur. For example, when van der Waals complexes such as HCl···Ar undergo so-called vibrational predissociation, one thinks in terms of movement of the Ar atom relative to the center of mass of the HCl molecule playing the role of the R coordinate above, and the vibrational state of HCl as playing the role of the quantized (electronic) state in the above example.

In such cases, a vibrationally excited HCl molecule (e.g., in v = 1) to which an Ar atom is attached via weak van der Waals attraction transfers its vibrational energy to the Ar atom, subsequently dropping to a lower (e.g., v = 0) vibrational level. Within the two-coupled-state model introduced above, the upper energy surface pertains to Ar in a bound vibrational level (having dissociation energy D_e) with HCl in an excited vibrational state (being the v = 0 to v = 1 vibrational energy gap), and the lower surface describes an Ar atom that is free from the HCl molecule that is itself in its v = 0 vibrational state. In this case, the coordinate R is the Ar-to-HCl distance.

In analogy with the electronic-nuclear coupling example discussed earlier, the rate of transition from HCl (v=1) bound to Ar to HCl(v=0) plus a free Ar atom depends on the strength of coupling between the Ar···HCl relative motion coordinate (R) and the HCl internal vibrational coordinate. The $<$ |d/dR| "$>$ coupling elements in this case are integrals over the HCl vibrational coordinate x involving the v = 0 ( ) and v = 1 (") vibrational functions. The integrals over the R coordinate in the earlier expression for the rate of radiationless transitions now involve integration over the distance R between the Ar atom and the center of mass of the HCl molecule.

This completes our discussion of dynamical processes in which more than one Born-Oppenheimer state is involved. There are many situations in molecular spectroscopy and chemical dynamics where consideration of such coupled-state dynamics is essential. These cases are characterized by

(i) total energies E which may be partitioned in two or more ways among the internal degrees of freedom (e.g., electronic and nuclear motion or vibrational and ad-atom in the above examples),

(ii) Born-Oppenheimer potentials that differ in energy by a small amount (so that energy transfer from the other degree(s) of freedom is facile).

III. Classical Treatment of Nuclear Motion

For all but very elementary chemical reactions (e.g., D + HH   HD + H or F + HH   FH + H) or scattering processes (e.g., CO (v,J) + He   CO (v',J') + He), the

above fully quantal coupled channel equations simply can not be solved even when modern supercomputers are employed. Fortunately, the Schrödinger equation can be replaced by a simple classical mechanics treatment of nuclear motions under certain circumstances.

For motion of a particle of mass μ along a direction R, the primary condition under which a classical treatment of nuclear motion is valid

$$\frac{1}{4} \frac{1}{p} \left| \frac{dp}{dR} \right| \ll 1$$

relates to the fractional change in the <u>local momentum</u> defined as:

$$p = \sqrt{2\mu(E - E_j(R))}$$

along R within the 3N - 5 or 3N - 6 dimensional internal coordinate space of the molecule, as well as to the <u>local de Broglie wavelength</u>

$$= \frac{2\, \hbar}{|p|} \quad .$$

The inverse of the quantity $\frac{1}{p} \left| \frac{dp}{dR} \right|$ can be thought of as the length over which the momentum changes by 100%. The above condition then states that the local de Broglie wavelength must be short with respect to the distance over which the potential changes appreciably. Clearly, whenever one is dealing with heavy nuclei that are moving fast (so |p| is large), one should anticipate that the local de Broglie wavelength of those particles may be short enough to meet the above criteria for classical treatment.

It has been determined that for potentials characteristic of typical chemical bonding (whose depths and dynamic range of interatomic distances are well known), and for all but low-energy motions (e.g., zero-point vibrations) of light particles such as Hydrogen and Deuterium nuclei or electrons, the local de Broglie wavelengths are often short enough for the above condition to be met (because of the large masses μ of non-Hydrogenic species) except when their velocities approach zero (e.g., near classical turning points). It is therefore common to treat the nuclear-motion dynamics of molecules that do not contain H or D atoms in a purely classical manner, and to apply so-called semi-classical corrections

near classical turning points. The motions of H and D atomic centers usually require quantal treatment except when their kinetic energies are quite high.

A. Classical Trajectories

To apply classical mechanics to the treatment of nuclear-motion dynamics, one solves Newtonian equations

$$m_k \frac{d^2 X_k}{dt^2} = - \frac{dE_j}{dX_k}$$

where X_k denotes one of the 3N cartesian coordinates of the atomic centers in the molecule, m_k is the mass of the atom associated with this coordinate, and $\frac{dE_j}{dX_k}$ is the derivative of the potential, which is the electronic energy $E_j(R)$, along the kth coordinate's direction. Starting with coordinates $\{X_k(0)\}$ and corresponding momenta $\{P_k(0)\}$ at some initial time $t = 0$, and given the ability to compute the force $- \frac{dE_j}{dX_k}$ at any location of the nuclei, the Newton equations can be solved (usually on a computer) using finite-difference methods:

$$X_k(t+\Delta t) = X_k(t) + P_k(t) \Delta t/m_k$$

$$P_k(t+\Delta t) = P_k(t) - \frac{dE_j}{dX_k}(t) \Delta t.$$

In so doing, one generates a sequence of coordinates $\{X_k(t_n)\}$ and momenta $\{P_k(t_n)\}$, one for each "time step" t_n. The histories of these coordinates and momenta as functions of time are called "**classical trajectories**". Following them from early times, characteristic of the molecule(s) at "reactant" geometries, through to late times, perhaps characteristic of "product" geometries, allows one to monitor and predict the fate of the time evolution of the nuclear dynamics. Even for large molecules with many atomic centers, propagation of such classical trajectories is feasible on modern computers if the forces - $\frac{dE_j}{dX_k}$ can be computed in a manner that does not consume inordinate amounts of computer time.

In Section 6, methods by which such force calculations are performed using first-principles quantum mechanical methods (i.e., so-called ab initio methods) are discussed. Suffice it to say that these calculations are often the rate limiting step in carrying out

classical trajectory simulations of molecular dynamics. The large effort involved in the <u>ab initio</u> determination of electronic energies and their gradients - $\dfrac{dE_j}{dX_k}$ motivate one to consider using empirical "force field" functions $V_j(R)$ in place of the <u>ab initio</u> electronic energy $E_j(R)$. Such model potentials $V_j(R)$, are usually constructed in terms of easy to compute and to differentiate functions of the interatomic distances and valence angles that appear in the molecule. The parameters that appear in the attractive and repulsive parts of these potentials are usually chosen so the potential is consistent with certain experimental data (e.g., bond dissociation energies, bond lengths, vibrational energies, torsion energy barriers).

For a large polyatomic molecule, the potential function V usually contains several distinct contributions:

$$V = V_{bond} + V_{bend} + V_{vanderWaals} + V_{torsion} + V_{electrostatic}.$$

Here V_{bond} gives the dependence of V on stretching displacements of the bonds (i.e., interatomic distances between pairs of bonded atoms) and is usually modeled as a harmonic or Morse function for each bond in the molecule:

$$V_{bond} = \sum_J 1/2 \, k_J \, (R_J - R_{eq,J})^2$$

or

$$V_{bond} = \sum_J D_{e,J} \, (1-\exp(-a_J(R_J - R_{eq,J})))^2$$

where the index J labels the bonds and the k_J, a_J and $R_{eq,J}$ are the force constant and equilibrium bond length parameters for the Jth bond.

V_{bend} describes the bending potentials for each triplet of atoms (ABC) that are bonded in a A-B-C manner; it is usually modeled in terms of a harmonic potential for each such bend:

$$V_{bend} = \sum_J 1/2 \, k_J \, (\theta_J - \theta_{eq,J})^2 \, .$$

The $\theta_{eq,J}$ and k_J are the equilibrium angles and force constants for the Jth angle.

$V_{vanderWaals}$ represents the van der Waals interactions between all pairs of atoms that are not bonded to one another. It is usually written as a sum over all pairs of such atoms (labeled J and K) of a Lennard-Jones 6,12 potential:

$$V_{vanderWaals} = \sum_{J<K} [a_{J,K} (R_{J,K})^{-12} - b_{J,K} (R_{J,K})^{-6}]$$

where $a_{J,K}$ and $b_{J,K}$ are parameters relating to the repulsive and dispersion attraction forces, respectively for the Jth and K^{th} atoms.

$V_{torsion}$ contributions describe the dependence of V on angles of rotation about single bonds. For example, rotation of a CH_3 group around the single bond connecting the carbon atom to another group may have an angle dependence of the form:

$$V_{torsion} = V_0 (1 - \cos(3\phi))$$

where ϕ is the torsion rotation angle, and V_0 is the magnitude of the interaction between the C-H bonds and the group on the atom bonded to carbon.

$V_{electrostatic}$ contains the interactions among polar bonds or other polar groups (including any charged groups). It is usually written as a sum over pairs of atomic centers (J and K) of Coulombic interactions between fractional charges $\{Q_J\}$ (chosen to represent the bond polarity) on these atoms:

$$V_{electrostatic} = \sum_{J<K} Q_J Q_K / R_{J,K}$$

Although the total potential V as written above contains many components, each is a relatively simple function of the Cartesian positions of the atomic centers. Therefore, it is relatively straightforward to evaluate V and its gradient along all 3N Cartesian directions in a computationally efficient manner. For this reason, the use of such empirical force fields in so-called **molecular mechanics** simulations of classical dynamics is widely used for treating large organic and biological molecules.

B. Initial Conditions

No single trajectory can be used to simulate chemical reaction or collisions that relate to realistic experiments. To generate classical trajectories that are characteristic of particular experiments, one must choose many initial conditions (coordinates and momenta)

the <u>collection</u> of which is representative of the experiment. For example, to use an **ensemble** of trajectories to simulate a molecular beam collision between H and Cl atoms at a collision energy E, one must follow many classical trajectories that have a range of "impact parameters" (b) from zero up to some maximum value b_{max} beyond which the H ····Cl interaction potential vanishes. The figure shown below describes the impact parameter as the distance of closest approach that a trajectory would have if no attractive or repulsive forces were operative.
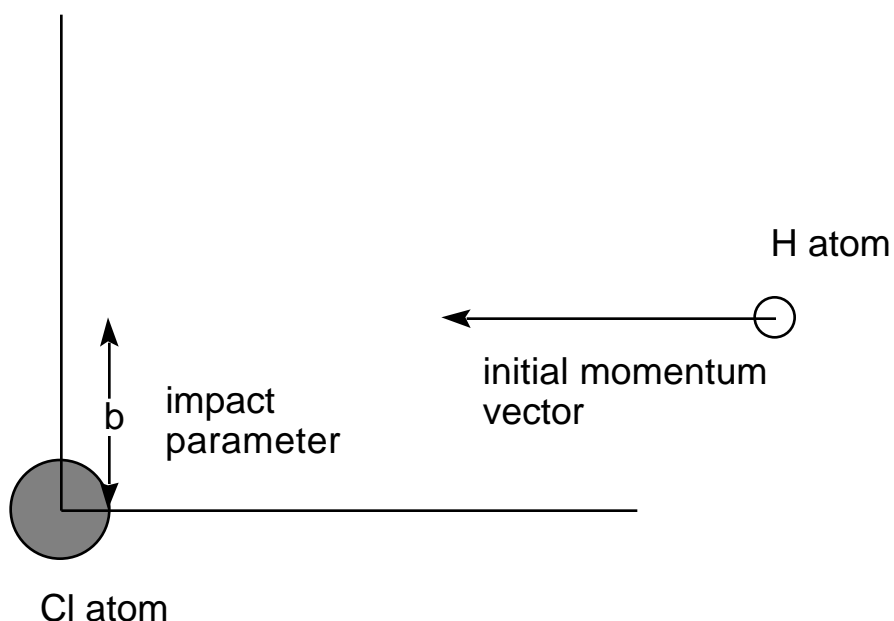
Moreover, if the energy resolution of the experiment makes it impossible to fix the collision energy closer than an amount E, one must run collections of trajectories for values of E lying within this range.

   If, in contrast, one wishes to simulate thermal reaction rates, one needs to follow trajectories with various E values and various impact parameters b from initiation at t = 0 to their conclusion (at which time the chemical outcome is interrogated). Each of these trajectories must have their outcome weighted by an amount proportional to a Boltzmann factor exp(-E/RT), where R is the ideal gas constant and T is the temperature because this factor specifies the probability that a collision occurs with kinetic energy E.

   As the complexity of the molecule under study increases, the number of parameters needed to specify the initial conditions also grows. For example, classical trajectories that relate to $F + H_2$ $HF + H$ need to be specified by providing (i) an impact parameter for the F to the center of mass of H_2, (ii) the relative translational energy of the F and H_2, (iii)

the radial momentum and coordinate of the H_2 molecule's bond length, and (iv) the angular momentum of the H_2 molecule as well as the angle of the H-H bond axis relative to the line connecting the F atom to the center of mass of the H_2 molecule. Many such sets of initial conditions must be chosen and the resultant classical trajectories followed to generate an ensemble of trajectories pertinent to an experimental situation.

It should be clear that even the classical mechanical simulation of chemical experiments involves considerable effort because no single trajectory can represent the experimental situation. Many trajectories, each with different initial conditions selected so they represent, as an ensemble, the experimental conditions, must be followed and the outcome of all such trajectories must be averaged over the probability of realizing each specific initial condition.

C. Analyzing Final Conditions

Even after classical trajectories have been followed from $t = 0$ until the outcomes of the collisions are clear, one needs to properly relate the fate of each trajectory to the experimental situation. For the $F + H_2 \quad HF + H$ example used above, one needs to examine each trajectory to determine, for example, (i) whether HF + H products are formed or non-reactive collision to produce $F + H_2$ has occurred, (ii) the amount of rotational energy and angular momentum that is contained in the HF product molecule, (iii) the amount of relative translational energy that remains in the H + FH products, and (iv) the amount of vibrational energy that ends up in the HF product molecule.

Because classical rather than quantum mechanical equations are used to follow the time evolution of the molecular system, there is no guarantee that the amount of energy or angular momentum found in degrees of freedom for which these quantities should be quantized will be so. For example, $F + H_2 \quad HF + H$ trajectories may produce HF molecules with internal vibrational energy that is not a half integral multiple of the fundamental vibrational frequency of the HF bond. Also, the rotational angular momentum of the HF molecule may not fit the formula J (J+1) $h^2/(8 \ ^2I)$, where I is HF's moment of inertia.

To connect such purely classical mechanical results more closely to the world of quantized energy levels, a method know as "binning" is often used. In this technique, one assigns the outcome of a classical trajectory to the particular quantum state (e.g., to a vibrational state v or a rotational state J of the HF molecule in the above example) whose quantum energy is closest to the classically determined energy. For the HF example at

hand, the classical vibrational energy $E_{cl,vib}$ is simply used to define, as the closest integer, a vibrational quantum number v according to:

$$v = \frac{(E_{cl,vib})}{\hbar} - 1/2.$$

Likewise, a rotational quantum number J can be assigned as the closest integer to that determined by using the classical rotational energy $E_{cl,rot}$ in the formula:

$$J = 1/2 \ \{ \ (1+32 \ ^2IE_{cl,rot}/h^2)^{1/2} -1 \}$$

which is the solution of the quadratic equation $J(J+1) h^2/8 \ ^2I = E_{cl,rot}$. By following many trajectories and assigning vibrational and rotational quantum numbers to the product molecules formed in each trajectory, one can generate histograms giving the frequency with which each product molecule quantum state is observed for the ensemble of trajectories used to simulate the experiment of interest. In this way, one can approximately extract product-channel quantum state distributions from classical trajectory simulations.

IV. Wavepackets

In an attempt to combine the attributes and stregths of classical trajectories, which allow us to "watch" the motions that molecules undergo, and quantum mechanical wavefunctions, which are needed if interference phenomena are to be treated, a hybrid approach is sometimes used. A popular and rather successful such point of view is provided by so called **coherent state wavepackets**.

A quantum mechanical wavefunction $(\mathbf{x}|\mathbf{X}, \mathbf{P})$ that is a function of all pertinent degrees of freedom (denoted collectively by $\mathbf{x}$) and that depends on two sets of parameters (denoted $\mathbf{X}$ and $\mathbf{P}$, respectively) is defined as follows:

$$(\mathbf{x}|\mathbf{X}, \mathbf{P}) = \sum_{k=1}^{N} (2 \ < \ x_k>^2)^{-1/2} \exp\{iP_k x_k/\hbar \ - \ (x_k-X_k)^2/(4< \ x_k>^2)\} \ .$$

Here, $< \ x_k>^2$ is the uncertainty

$$< \ x_k>^2 = \int | \ |^2 (x_k-X_k)^2 d\mathbf{x}$$

along the kth degree of freedom for this wavefunction, defined as the mean squared displacement away from the average coordinate

$$\int |\ |^2 x_k d\mathbf{x} \ = X_k.$$

So, the parameter X_k specifies the <u>average value</u> of the coordiate x_k. In like fashion, it can be shown that the parameter P_k is equal to the <u>average value</u> of the momentum along the kth coordinate:

$$\int \ ^*(-i\hbar\ \partial/\partial x_k\ \ )d\mathbf{x} \ = P_k.$$

The uncertainty in the momentum along each coordinate:

$$<\ p_k>^2 = \ \int \ ^*(-i\hbar\ \partial/\partial x_k - P_k)^2\ \ d\mathbf{x}$$

is given, for functions of the coherent state form, in terms of the coordinate uncertainty as

$$<\ p_k>^2 <\ x_k>^2 = \hbar^2/4.$$

Of course, the general Heisenberg uncertainty condition

$$<\ p_k>^2 <\ x_k>^2 \ \geq \hbar^2/4$$

limits the coordinate and momentum uncertainty products for arbitrary wavefunctions. The coherent state wave packet functions are those for which this <u>uncertainty</u> product <u>is minimum</u>. In this sense, coherent state wave packets are seen to be as close to classical as possible since in classical mechanics there are no limits placed on the resolution with which one can observe coordinates and momenta.

These wavepacket functions are employed as follows in the most straightforward treatements of combined quantal/classical mechanics:

1. Classical trajectories are used, as discribed in greater detail above, to generate a series of coordinates $X_k(t_n)$ and momenta $P_k(t_n)$ at a sequence of times denoted $\{t_n\}$.

2. These classical coordinates and momenta are used to <u>define</u> a wavepacket function as written above, whose X_k and P_k parameters are taken to be the coordinates and momenta of the classical trajectory. In effect, the wavepacket moves around "riding" the classical trajectory's coordiates and momenta as time evolves.

3. At any time t_n, the quantum mechanical properties of the system are computed by forming the expectation values of the corresponding quantum operators for a wavepacket wavefunction of the form given above with X_k and P_k given by the classical coordinates and momenta at that time t_n.

Such wavepackets are, of course, simple approximations to the true quantum mechanical functions of the system because they do not obey the Schrödinger equation appropriate to the system. The should be expected to provide accurate representations to the true wavefunctions for systems that are more classical in nature (i.e., when the local de Broglie wave lengths are short compared to the range over which the potentials vary appreciably). For species containing light particles (e.g., electrons or H atoms) or for low kinetic energies, the local de Broglie wave lengths will not satisfy such criteria, and these approaches can be expected to be less reliable. For further information about the use of coherent state wavepackets in molecular dynamics and molecular spectroscopy, see E. J. Heller, Acc. Chem. Res. <u>14</u>, 368 (1981).

This completes our treatment of the subjects of molecular dynamics and molecular collisions. Neither its depth not its level was at the research level; rather, we intended to provide the reader with an introduction to many of the theoretical concepts and methods that arise when applying either the quantum Schrödinger equation or classical Newtonian mechanics to chemical reaction dynamics. Essentially none of the experimental aspects of this subject (e.g., molecular beam methods for preparing "cold" molecules, laser pump-probe methods for preparing reagents in specified quantum states and observing products in such states) have been discussed. An excellent introduction to both the experimental and theoretical foundations of modern chemical and collision dynamics is provided by the text <u>Molecular Reaction Dynamics and Chemical Reactivity</u> by R. D. Levine and R. B. Bernstein, Oxford Univ. Press (1987).